Available online at www.sciencedirect.com
ScienceDirect
Biochimica et Biophysica Acta 1768 (2007) 715–727
Biochimica et Biophysica Acta BBA
www.elsevier.com/locate/bbamem

Effects of topology, length, and charge on the activity of a kininogen-derived peptide on lipid membranes and bacteria

Lovisa Ringstad [a], Lukasz Kacprzyk [b,c], Artur Schmidtchen [c], Martin Malmsten [a,*]

[a] Department of Pharmacy, Uppsala University, P.O. Box 580, SE-751 23 Uppsala, Sweden
[b] Department of Microbiology, Faculty of Biochemistry, Biophysics and Biotechnology, Jagiellonian University, ul. Gronostajowa 7, 30-387 Krakow, Poland
[c] Section of Dermatology and Venereology, Department of Clinical Sciences, Lund University, Biomedical Center, Tornavägen 10, SE-221 84 Lund, Sweden

Received 29 September 2006; received in revised form 3 November 2006; accepted 29 November 2006
Available online 15 December 2006

Abstract

Effects of topology, length, and charge on peptide interactions with lipid bilayers was investigated for variants of the human kininogen-derived peptide HKH20 (HKHGHGHGKHKNKGKKNGKH) by ellipsometry, CD, fluorescence spectroscopy, and z-potential measurements. The peptides display primarily random coil conformation in buffer and at lipid bilayers, and their lipid interaction is dominated by electrostatics, the latter evidenced by higher peptide adsorption and resulting membrane rupture for an anionic than for a zwitterionic membrane, as well as by strongly reduced adsorption and membrane rupture at high ionic strength. At sufficiently high peptide charge density, however, electrostatic interactions contribute to reducing the peptide adsorption and membrane defect formation. Truncating HKH20 into overlapping 10 amino acid peptides resulted in essentially eliminated membrane rupture and in a reduced amount peptide charges pinned at the lipid bilayer. Finally, cyclic HKH20 was found to be less efficient than the linear peptide in causing liposome rupture, partly due to a lower adsorption. Analogous results were found regarding bactericidal effects.

Keywords: Adsorption; Antimicrobial; Bacteria; Ellipsometry; Liposome; Membrane; Peptide

1. Introduction

In the wake of growing bacteria resistance development, there is significant current interest in identifying new types of antibiotics [1,2]. One class of substances which has received interest in this context are antimicrobial peptides (AMPs) [3–23]. Such AMPs have been identified from a number of sources, including plants [12,13] and insects [14], and significant interest is currently directed towards AMPs of endogenous origin [3–6,15–19]. Although there is increasing evidence that AMPs influence bacteria in a multitude of ways, it is believed that bacterial wall rupture plays a key role in the bactericidal action of AMPs [3–6,20]. Given this, limited bacterial resistance development towards AMPs is expected [21–23].

A major challenge in identifying AMPs for potential therapeutic use is the AMP selectivity between bacteria and eukaryotic cells, such that bacterial walls are ruptured whereas effects on eukaryotic cells, and resulting cytotoxicity, is low. Several peptides displaying such selectivity are currently being developed for therapeutic use [3–5]. We have contributed to the identification of novel such selective antimicrobial peptides, e.g., from the human complement peptide C3a [17], kininogen [18], and matrix proteins [19]. One such previously identified peptide, which has been found to be promising at least for topical use is HKH20, a peptide derived from domain 5 of human high molecular weight kininogen. This peptide, which was previously investigated in some detail [18], also has the added advantage of not being readily degradable by common bacterial elastases.

In the present investigation, we continue examining the action of this latter peptide from a mechanistic perspective, notably regarding the role of peptide surface activity on the interaction of this peptide with lipid bilayers and bacteria. In doing so, we also investigate the effect of peptide topology, length, and electrostatic interactions with fluorescence spectroscopy, circular dichroism, z-potential measurements, and *in situ* ellipsometry.

* Corresponding author. Fax: +46 18 471 4377.
E-mail address: martin.malmsten@farmaci.uu.se (M. Malmsten).

0005-2736/$ - see front matter © 2006 Elsevier B.V. All rights reserved.
doi:10.1016/j.bbamem.2006.11.016

2. Experimental

2.1. Materials

The peptides investigated in the present study (Table 1) were synthesized by Innovagen AB, Sweden, and were all of >95% (in most cases >98%) purity as indicated by HPLC and MALDI-TOF analysis (Voyager, Applied Biosystems). The primary source of impurity is peptides with one or several amino acids deleted. Overall, this relative minuteness and type of impurities is not expected to affect the interpretation of the data. 1,2-Dioleoyl-*sn*-Glycero-3-Phosphate (DOPA) (monosodium salt) and 1,2-dioleoyl-*sn*-Glycero-3-phoshocholine (DOPC) were both from Avanti Polar Lipids (Alabaster, USA) and of >99% purity, while cholesterol of >99% purity, calcein of >97% purity, n-dodecyl-β-D-maltoside (DDM) of ≥98% purity, Triton X-100, and poly-L-lysine (M_w = 59 kDa and 170 kDa) were all from Sigma-Aldrich (St. Louis, USA). Finally, 5(6)-carboxyfluorescein (CF) of 99% purity was from Acros Organics (New Jersey, USA). All other chemicals were of analytical grade, and water used was of Millipore Milli-Q Plus 185 ultra-pure quality.

2.2. Surfaces

Silica surfaces for ellipsometry were prepared from polished silicon slides (Okmetic, Vantaa, Finland), which were oxidized to an oxide layer thickness of 30 nm. These surfaces were then cleaned first in 25% NH_4OH, 30% H_2O_2, and H_2O (1:1:5, by volume), and then again in 32% HCl, 30% H_2O_2, and H_2O (1:1:5, by volume), both at 80 °C for 5 min. This treatment renders the surfaces highly hydrophilic. The surfaces were then stored in 95% ethanol. Immediately prior to use, the surfaces were plasma treated for 5 min at 18 W in low pressure residual air (0.2 mbar) in a Harrick Plasma Cleaner, PDC-32G, (Harrick Scientific Corp, Ithaca, USA).

2.3. Microorganisms

Escherichia coli, isolate 25922, and *Staphylococcus aureus*, isolate 29213, were both obtained from The American Type Culture Collection (ATCC, Rockville, MD, USA). *Pseudomonas aeruginosa,* isolate 15159, *Escherichia coli*, isolate 37.4, and *Staphylococcus aureus*, isolate 1, were all clinical isolates obtained from wound (*E. coli, P. aeruginosa*) and skin (*S. aureus*) infections (Department of Bacteriology, Lund University).

2.4. Radial diffusion assay

Radial diffusion assay (RDA) was performed as described previously [24]. Bacteria were grown to mid-logarithmic phase in 10 ml of 3% w/v trypticase soy broth (TSB) (Becton-Dickinson, Cockeysville, USA). After this, they were washed in 10 mM buffer (sodium acetate, pH 5.5, MES (2-morpholinoethanesulfonic acid), pH 5.5, Tris (tris(hydroxymethyl) aminomethane hydrochloride), pH 7.4, or PIPES (piperazine-*N,N′*-bis(ethanesulfonic acid), pH 7.4), and 4×10^6 bacterial cfu was added to 5 ml of the underlay agarose gel, consisting of 1% (w/v) low-electroendosmosis (Low-EEO) type agarose, 0.02% (v/v), Tween 20 (Sigma-Aldrich, St. Louis, USA), and 0.03% (w/v) TSB. The underlay was poured into Ø 85 mm petri dishes. After agarose solidification, 4 mm-diameter wells were punched in the underlay, and 6 μl samples were added to the wells then formed. The plates were then incubated at 37 °C for 3 h to allow peptide diffusion, after which the underlay gel was covered with 5 ml of molten overlay (6% TSB and 1% Low-EEO agarose in dH_2O), and the peptide antimicrobial activity visualized as a clear zones around each well after 18–24 h of incubation at 37 °C. The results from these experiments are given as mean diameters (n = 3) of the clear zones formed for the different peptides.

2.5. Viable count analysis

S. aureus and *E. coli* were grown to mid-logarithmic phase in Todd–Hewitt (TH) medium. Bacteria were washed and diluted in either 10 mM Tris, pH 7.4, containing 5 mM glucose, or 10 mM MES buffer, pH 5.5. Bacteria (50 μl; 2×10^6 bacteria/ml) were then incubated for 2 h at 37 °C. Serial dilutions of the incubation mixture were plated on TH agar, followed by incubation at 37 °C overnight, after which the number of colony-forming units (cfu) was determined.

Table 1
Structure and properties of the peptides investigated

HKHGHGHGKHKNKGKKNGKH	(HKH20)
HKHGHGHGKH	(HKH10)
GHGKHKNKGK	(GHG10)
KNKGKKNGKH	(KNK10)
CHKHGHGHGKHKNKGKKNGKHC	(CHK22 l)
HKHGHGHGKHKNKGKKNGKH	(CHK22 c)
C——————————C	

	HKH20	HKH10	GHG10	KNK10	CHK22
IP[1]	11.2	10.5	10.9	11.0	11.2
Znet[2] (pH 7.4)	+6	+3	+4	+4	+6
Znet (pH 5.5)	+12	+6	+6	+6	+12
H[3]	−0.77	−0.51	−0.81	−1.03	−0.70

[1]IP: isoelectric point; [2]Z_{net}: net charge; [3]H: mean hydrophobicity on the Eisenberg scale.

2.6. Lactate dehydrogenase (LDH) assay

HaCaT keratinocytes were grown in 96 well plates (3000 cells/well) in serum free keratinocyte medium (SFM) supplemented with bovine pituitary extract and recombinant EGF (BPE-rEGF) (Invitrogen, USA) to confluency. The medium was then removed, and 100 μl of the peptides investigated (at 60 μM, diluted in SFM/BPE-rEGF) were added in triplicates to different wells of the plate. The LDH based TOX-7 kit (Sigma-Aldrich, St. Louis, USA) was used for quantification of LDH release from the cells. Results given represent mean values from triplicate measurements. Results are given as fractional LDH release compared to the positive control consisting of 1% Triton X-100 (yielding 100% LDH release).

2.7. MTT assay

Sterile filtered MTT (3-(4,5-dimethylthiazolyl)-2,5-diphenyl-tetrazolium bromide; Sigma-Aldrich) solution (5 mg/ml in PBS) was stored protected from light at −20 °C until usage. HaCaT keratinocytes, 3000 cells/well, were seeded in 96 well plates and grown in keratinocyte-SFM/BPE-rEGF medium to confluency. Peptides investigated were then added at 60 μM. After incubation over night, 20 μl of the MTT solution was added to each well and the plates incubated for 1 h in CO_2 at 37 °C. The MTT containing medium was then removed by aspiration. The blue formazan product generated was dissolved by the addition of 100 μl of 100% DMSO per well. The plates were then gently swirled for 10 min at room temperature to dissolve the precipitate. The absorbance was monitored at 550 nm, and results given represent mean values from triplicate measurements.

2.8. Hemolysis

EDTA-blood was centrifuged at 800×*g* for 10 min, after which plasma and buffy coat were removed. The erythrocytes were then washed three times and resuspended in PBS, pH 7.4. After this, the cells were incubated with end-over-end rotation for 1 h at 37 °C in the presence of 60 μM peptide. 2% Triton X-100 (Merck, Stockholm, Sweden) served as positive control. The samples were then centrifuged at 800×*g* for 10 min. The absorbance of hemoglobin release was measured at 540 nm and is in the plot expressed as % of TritonX-100 induced hemolysis. As negative control, the spontaneous leakage of hemoglobin during the same procedure was used. Results given represent mean values from triplicate measurements.

2.9. Liposome preparation

The liposomes investigated in the present study were either zwitterionic (DOPC/cholesterol 60/40 mol/mol) or anionic (DOPC/DOPA/cholesterol 30/30/40 mol/mol). Due to their long, symmetric and unsaturated acyl chains, several methodological advantages are reached with these phospholipids. First, membrane cohesion is good, which facilitates quite stable liposomes and well defined supported lipid bilayers. Furthermore, the charge density of the lipid surface can be varied without domain formation. This substantially facilitates the interpretation of the observed peptide effects since domain formation in the mixed phospholipid system, as well as preferential peptide adsorption at domain fringes, can be excluded. If the aim would have been to mimic bacterial lipid membranes in detail, cholesterol should be excluded, and the liposome chain length and saturation altered to more closely adhere to species-specific bacterial lipid membrane compositions, as should the phospholipid headgroup. However, apart from the technical reasons given above, our aim with the anionic and the zwitterionic liposomes was *not* to mimic bacteria and eukaryotic cell membranes, respectively, but merely to monitor the effects of electrostatics on the lipid–peptide interaction, as we did also by varying the ionic strength and the peptide charge density. Cholesterol, although "non-biological" in the context of bacteria, was initially added merely to reduce spontaneous leakage from the liposomes to less than a few % during the time-scale of the experiment, in an effort to provide the highest possible quality of the leakage data. Given these differences between the presently used lipid model membranes and those of bacteria and eukaryotic cells, however, one should be aware that information on system-specific aspects of the interaction between the peptides and lipid membranes in bacteria and eukaryotic cells may not be fully available from investigations of these model lipid systems (as is the case with any model lipid systems).

In either case, the phospholipid(s) were dissolved in chloroform together with cholesterol, after which the solvent was evaporated under vacuum for 45 min at 60 °C, and subsequently in a vacuum oven (Lab-line, Melrose Park, USA) at 30 in-Hg and room temperature over night. Following drying, the thin lipid film formed at the wall of the glass container was resuspended in either 100 mM 5(6)-carboxyflourescein (CF) or 100 mM calcein in either 10 mM Tris buffer, pH 7.4, with or without additional 150 mM NaCl, or 10 mM sodium acetate buffer, pH 5.5. The solutions were then subjected to eight freeze–thaw cycles, each cycle involving first freezing in liquid nitrogen, then heating to 60 °C while vortexing. Unilamellar liposomes, largely free of multilamellar structures and incomplete liposomes, and of about 140 nm diameter, were generated by repeated extrusion through 100 nm polycarbonate membranes mounted in a LipoFast Basic extruder (Avestin, Mannheim, Germany). The liposomes thus generated were separated from untrapped CF or calcein by running the sample on a Sephadex™ G-25 column (Amersham Biosciences, Uppsala, Sweden) with either Tris or acetate buffer as eluent.

2.10. Liposome leakage

Liposome leakage and CF or calcein release was monitored at 37 °C by a A Spex fluorolog 1680 0.22 m double spectrometer (Instruments S.A. Group, Edison, USA), following the emitted fluorescence at 520 nm (CF) or 522 nm (calcein) from a

liposome dispersion (10 mM lipid in 10 mM Tris pH 7.4, or 10 mM sodium acetate, pH 5.5, either with or without 150 mM NaCl added). By disrupting the liposomes at the end of the experiment through addition of 0.05 wt.% Triton X-100, 100% release and an absolute leakage scale is obtained. All measurements were performed in at least duplicate.

2.11. Peptide secondary structure

Peptide secondary structure was monitored in the range 190–260 nm at 37 °C by circular dichroism (CD) using a Jasco J-810 Spectropolarimeter (Jasco, Tokyo, Japan). Measurements were performed under stirring in a quartz cuvette at a peptide concentration of 10 μM, both in buffer and in the presence of liposomes, the latter at a lipid concentration of 100 μM. The fraction of α-helical conformation was calculated from the recorded CD signal at 225 nm and those of reference peptides in purely helical and random coil conformations, respectively [25,26]. All α-helix and all random coil references were obtained from 0.133 mM (monomer concentration) poly-L-lysine (M_w=79 kDa) in 0.1 M NaOH and 0.1 M HCl, respectively. Background subtraction was performed routinely, and signals from the bulk solution were corrected for.

2.12. Peptide adsorption

Peptide adsorption to supported lipid bilayers was studied *in situ* by null ellipsometry [27], using an Optrel Multiskop (Optrel, Kleinmachnow, Germany) equipped with a 100 mW argon laser. All measurements were performed at 532 nm and an angle of incidence of 67.66° in a 5 ml cuvette under stirring (300 rpm). By monitoring the change in polarization of light reflected at a surface in the absence and presence of an adsorbed layer, the mean refractive index (n) and layer thickness (d) of the adsorbed layer can be obtained. From the thickness and refractive index the adsorbed amount (Γ) was calculated according to de Feijter [28], using a refractive index increment of 0.154 cm^3/g. Corrections were done routinely for changes in bulk refractive index caused by changes in temperature and excess electrolyte concentration.

Zwitterionic bilayers were deposited as described in detail previously [29,30]. In brief, a mixed micellar solution containing 60/40 mol/mol DOPC/cholesterol and DDM was prepared by addition of 19 mM DDM in water to DOPC/cholesterol dry lipid films, followed by stirring over night, yielding a solution containing 97.3 mol% DDM, 1.6 mol% DOPC, and 1.1 mol% cholesterol. The resulting solution was added to the cuvette at 25 °C, and the resulting adsorption monitored. When adsorption had stabilised, rinsing with water at 5 ml/min was initiated to remove mixed micelles from solution and surfactant from the substrate. By repeating this procedure and subsequently lowering the concentration of the micellar solution stable, densely packed bilayers are formed, with structural characteristics similar to those of bulk lamellar structures of the lipids [29].

As sub-bilayer adsorption resulted from the above mixed micelle approach in the case of the anionic lipid mixture, supported bilayers were generated from liposome adsorption in this case. DOPA/DOPC/cholesterol liposomes (30/30/40 mol/mol) were prepared as described above, but the dried lipid films resuspended in Tris buffer containing no CF or calcein. In order to avoid peptide adsorption directly at the silica substrate through any defects of the supported lipid layer, poly-L-lysine (M_w=170 kDa) was preadsorbed from water prior to liposome addition to an amount of 0.045±0.01 mg/m^2, followed by removal of nonadsorbed poly-L-lysine by rinsing with water at 5 ml/min for 20 min. Water in the cuvette was then replaced by buffer containing also 150 mM NaCl, which was followed by addition of liposomes in buffer at a lipid concentration of 20 μM. This was followed by rinsing with buffer (5 ml/min for 15 min) when the liposome adsorption had stabilised. The final layer formed had structural characteristics (thickness 40±10 Å, mean refractive index 1.47±0.026) similar to those of the zwitterionic bilayers, which suggests that a layer fairly close to a complete bilayer is formed. Again, the bilayer build-up was performed at 25 °C.

After lipid bilayer formation the temperature was raised to 37 °C and the cuvette content replaced by buffer at a rate of 5 ml/min over a period of 30 min. After this, the surface was allowed to stabilise for 40 min, after which peptide was added, first to a concentration of 0.01 μM, then to 0.1 μM, 0.5 μM and 1 μM, respectively, in all cases monitoring the adsorption for 1 h. All measurements were made in at least duplicate.

2.13. Liposome electrostatic potential

The z-potential of the liposomes with and without added peptides was determined by measuring the electrophoretic mobility using a Zetasizer Nano ZS (Malvern Instruments Ltd., UK). Measurements were performed at 25 °C (due to air bubbles precluding measurements at 37 °C) in disposable Zeta cells (Malvern Instruments Ltd., UK). The lipid concentrations used were 40 μM for zwitterionic liposomes and 20 μM for anionic liposomes, respectively. These concentrations were chosen in order to obtain a count rate sufficiently high for the measurements. Peptide to lipid ratios were chosen to be identical to those used in the leakage experiments. All measurements were done in at least triplicate 1 h after sample preparation.

3. Results and discussion

As indicated above, HKH20 represents an interesting type of antimicrobial peptide for several reasons. First, degradation of high molecular weight kininogen (HMWK) by neutrophil-derived proteases, as well as by the metalloproteinase elastase from *P. aeruginosa*, yield fragments containing HKH20 epitopes [18]. Hence, HKH20 is an endogenous peptide formed by proteases occurring during inflammation, which is not rapidly degraded further by bacterial proteolytic enzymes. Furthermore, HKH20 and analogues thereof display broad spectrum antibacterial properties, and simultaneous low toxicity. As an illustration of this, Fig. 1 compares the antibacterial potency of HKH20 with the benchmark LL37 peptide, while

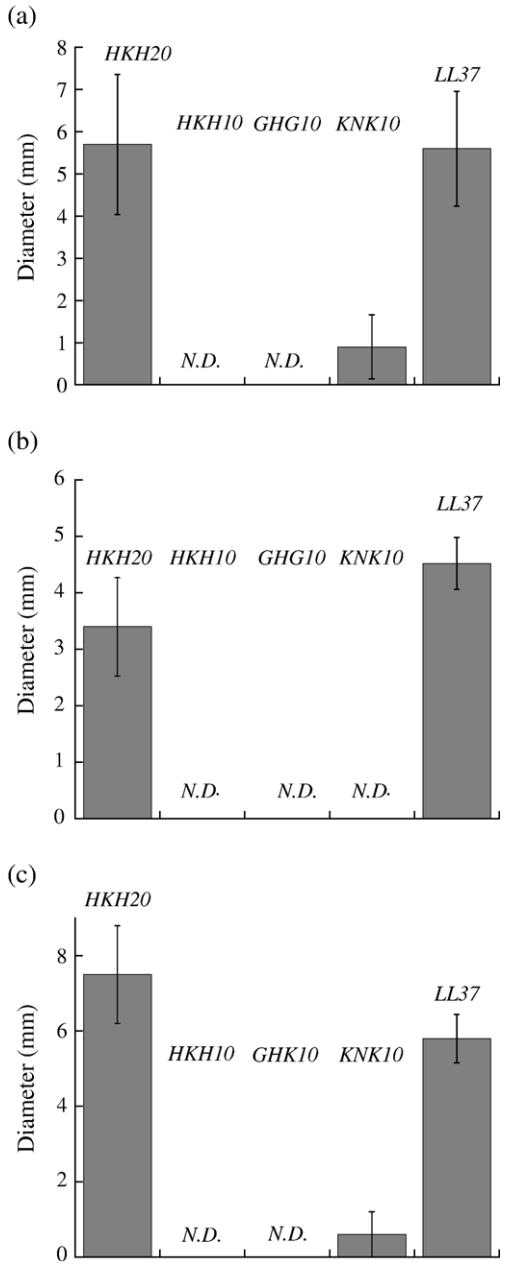

Fig. 1. Bactericidal activity of HKH20 variants and the extensively studied benchmark peptide LL37 against *P. aeruginosa* 15159 (a), *S. aureus* 1 (b), and *E. coli* 37.4 (c) determined by RDA at a peptide concentration of 60 μM in 10 mM Tris, pH 7.4. The higher the diameter, the higher the bacterial growth inhibition. N.D. refers to no detectable inhibition zone.

Fig. 2 shows results obtained regarding three toxicity-related effects, i.e., hemolysis, LDH release, and cellular viability (MTT assay). As can be seen, HKH20 displays an antibacterial effect comparable to that of the potent benchmark LL37 for a number of bacterial strains, at the same time as toxicity towards erythrocytes and keratinocytes is much lower for the HKH20 analogues investigated, bordering to being undetectable with the concentrations and assays employed. It should be noted here, however, that the cellular toxicity illustrated presently for LL37 does not necessarily disqualify this peptide from being therapeutically interesting. Instead, this peptide displays quite strong antibacterial effects, also at high ionic strength, as well as a range of other potentially interesting properties, e.g., relating to LPS neutralization, chemotactic activity, promotion of re-epithelization, and wound closure [23], and toxicity effects observed for the native peptide may be reduced at largely maintained antimicrobial and LPS binding properties by peptide truncation [23]. It should also be emphasized, that in the present investigation, focus is *not* placed on the possible therapeutic aspects of HKH20 or variants thereof, but rather on how variations in electrostatic interactions, peptide length and topology affect the interaction between the peptide and model

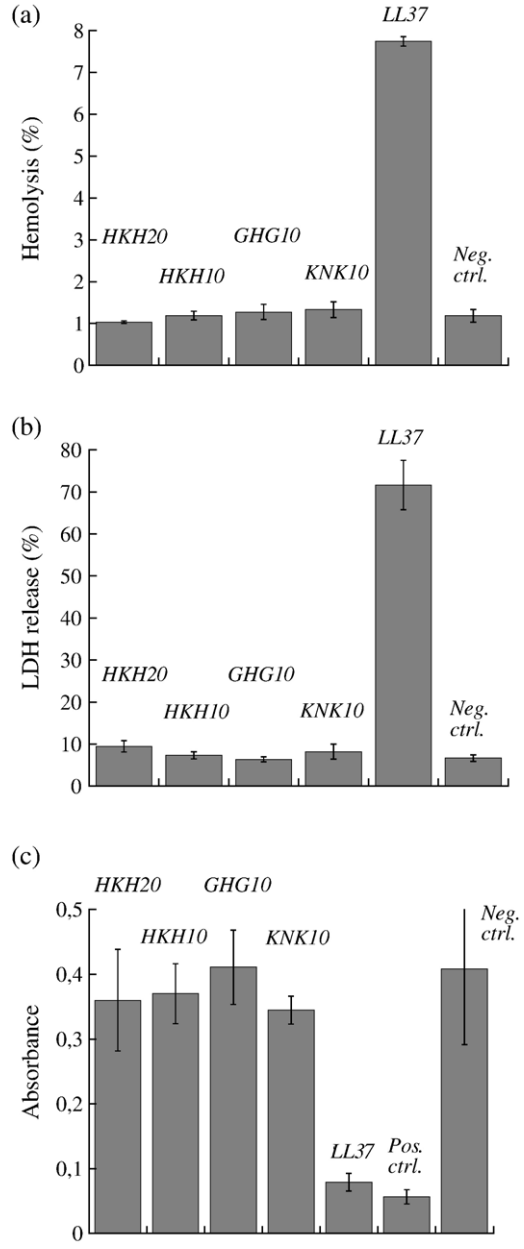

Fig. 2. Peptide-induced effects of HKH20 variants and of the extensively studied benchmark peptide LL37 in terms of hemolysis (a), LDH release (b), and MTT viability assay (c) at a peptide concentration of 60 μM. The absorbance for the positive and negative control in the hemolysis was 4.96±0.085 and 0.11±0.01, respectively.

lipid bilayers, as well as the antibacterial properties of HKH20 variants.

As shown in Figs. 1, 3 and 4), HKH20 is potent both against Gram positive *S. aureus* and Gram negative *E. coli* and *P. aeruginosa* bacterial isolates. Truncating the peptide into half its original length, i.e., 10 amino acids, however, results in a drastic reduction in bactericidal activity for all the bacteria strains investigated, irrespectively if the truncated 10 amino acid peptide is from the C-terminus, the N-terminus or the middle segment of the original HKH20 peptide (Fig. 1). An analogous peptide length dependence can be seen in liposome leakage induced by HKH20 and the truncated peptides. Thus, as can be seen in Fig. 5, the truncations all show non-detectable liposome leakage induction for both anionic and zwitterionic liposomes, whereas HKH20 is efficient in leakage induction in both types of liposomes.

Perhaps not entirely surprising given the high net charge (+6) and the relatively hydrophilic nature (H=−0.77 on the Eisenberg scale) of HKH20, electrostatic interactions play a central role in the interaction between HKH20 and lipid bilayers. Thus, leakage induction is significantly higher for the anionic than for the zwitterionic liposomes, and the capacity to cause liposome leakage is strongly decreased at high excess electrolyte concentration (Fig. 5). The latter effect is seen also in bacterial killing (displaying >95% reduction in bactericidal effect in the additional presence of 150 mM NaCl; results not shown). An interesting observation relating to the role of electrostatic interactions in liposome leakage induction can also be made by comparing Fig. 5a and c. Thus, while leakage induction is comparable for the two leakage probes CF and calcein in the case of the zwitterionic liposome, HKH20-induced liposome leakage for anionic liposome is significantly higher for the monovalently negatively charged CF than for the trivalently negatively charged calcein. Since the two fluorescent markers are of very similar size and identical aromatic ring structure, the results suggest that the leakage of the higher

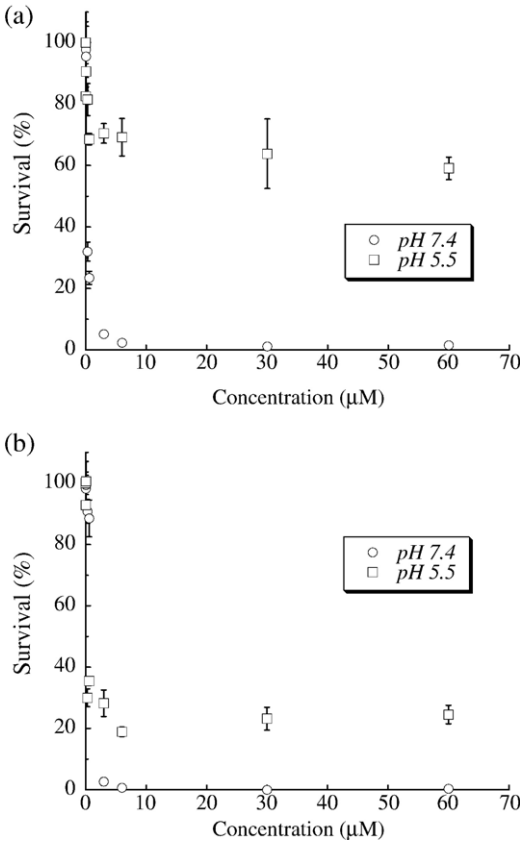

Fig. 3. Viable count analysis of the antibacterial effect of HKH20 on *S. aureus* 29213 (a) and *E. coli* 25922 (b) in 10 mM Tris, pH 7.4 and 10 mM MES, pH 5.5.

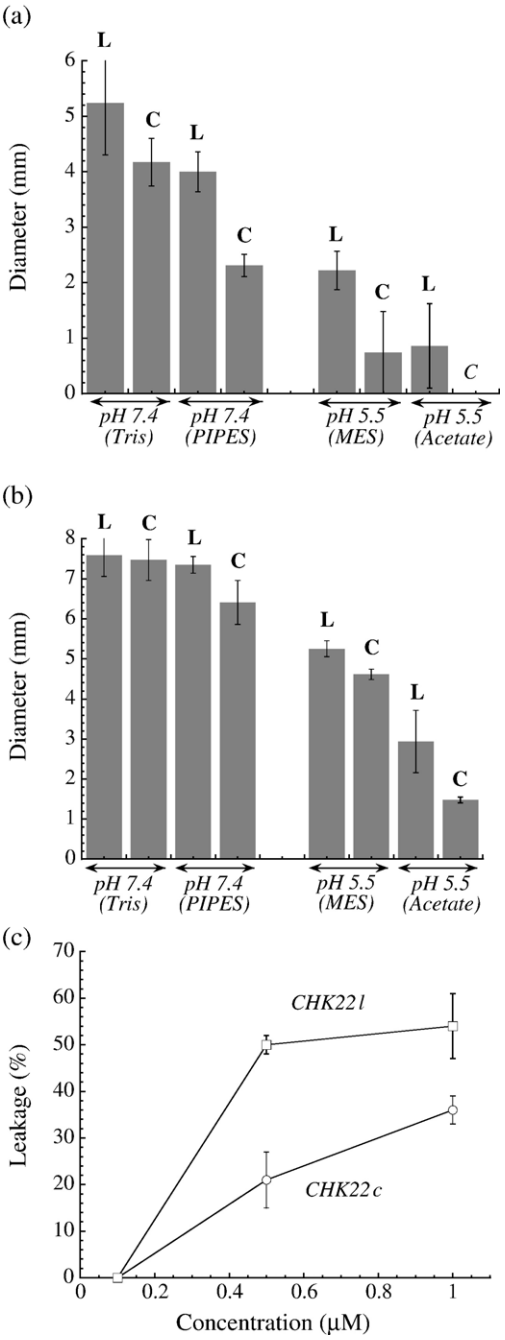

Fig. 4. RDA results for CHK22 l ("L") and CHK22 c ("C") with *S. aureus* 29213 (a) and *E. coli* 25922 (b) from 10 mM buffer at pH 5.5 and 7.4. The peptide concentration was 100 μM throughout. Shown also in (c) is CF liposome leakage induced by CHK22 l and CHK22 c for DOPC/DOPA/cholesterol (30/30/40) in 10 mM Tris, pH 7.4.

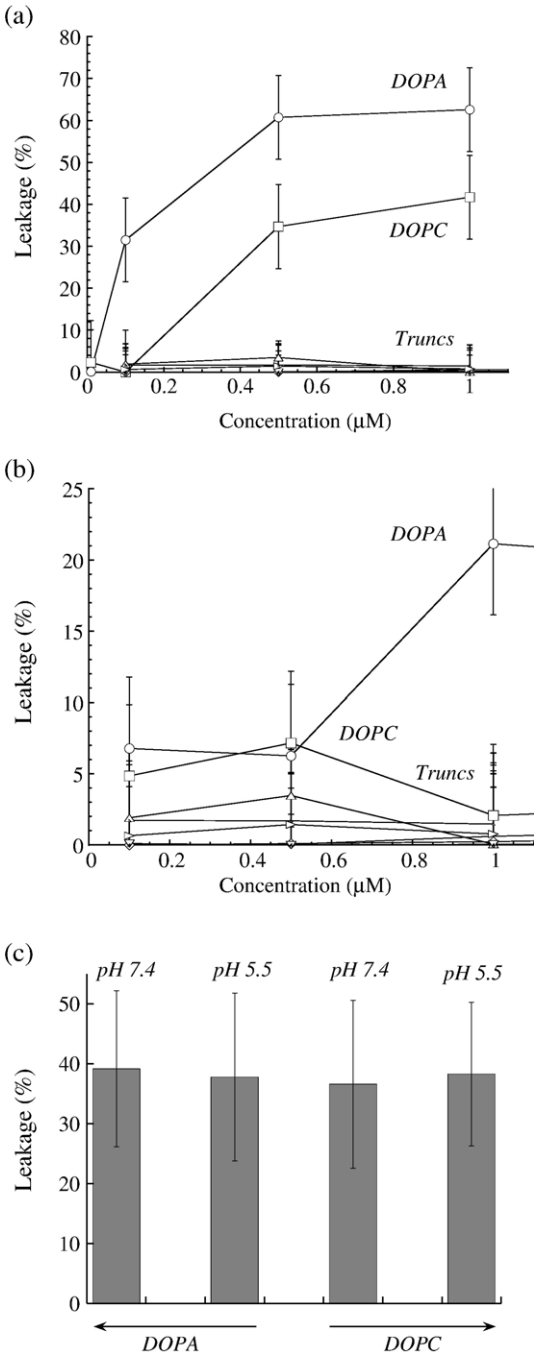

Fig. 5. CF liposome leakage induced by HKH20 and its truncated decapeptides HKH10, KNK10 and GHG10 for DOPC/cholesterol (60/40) ("DOPC") and DOPC/DOPA/cholesterol (30/30/40) ("DOPA") without (a) and with (b) additional 150 mM NaCl. For the truncated peptides, only results obtained for DOPC/DOPA/cholesterol (30/30/40) are shown for clarity (open triangles: HKH10, reverse open triangles: GHG10, open arrows: KNK10). (c) Effect of pH on calcein liposome leakage caused by addition of 1 μM HKH20.

charged calcein is reduced in the case of DOPA due to electrostatic interactions with net positively charged HKH20 positioned around the membrane defects. The reason for not the same happening in the case of DOPC may then be related to the lower peptide adsorption density for the latter system (see below). Ideally, one would like to investigate this further by comparing CF and calcein leakage also at high electrolyte concentration, where partial calcein pinning by oppositely charged HKH20 around defects should be reduced. However, since leakage induction at these conditions is non-measurable due to strongly reduced leakage induction of HKH20 and reduced peptide adsorption (see below), such investigations are not possible. We are currently extending these investigations to additional modified HKH peptides, and hope to be able to investigate these effects further in this context, which however is the subject of a separate communication and outside the scope of the present investigation.

As seen in Fig. 4, also the topology of the peptide is important to its effects on bacteria and liposomes. Hence, cyclicized C-HKH20-C is less efficient in causing liposome leakage than the corresponding linear variant, and also displays a reduced antibacterial effect, most clearly seen for *S. aureus*.

Secondary structure transitions on peptide binding and incorporation to lipid membranes, and notably formation of helix bundles or similar structures, have previously been found to be central in the membrane rupture caused by some antimicrobial peptides [4–11]. We therefore probed the secondary structure of HKH20 and its truncation and topology variants both in buffer and in liposome solutions. As can be seen in Fig. 6, all peptides investigated are characterized by primarily random coil conformation both in buffer and when bound to both anionic and zwitterionic liposomes. Hence, ordered secondary structures do not seem to play a significant role in the membrane rupture caused by HKH20 and its variants.

A factor, however, which does play an important role in membrane defect formation is the adsorption density of the peptide at the lipid bilayer. Shown in Figs. 7–9 are results obtained by *in situ* ellipsometry on the adsorption of HKH20, HKH10, CHK22 l and CHK22 c at well-defined supported phospholipid bilayers. As can be seen, the peptide adsorption can be straightforwardly monitored as a function of time, and binding isotherms obtained. Supporting the results obtained on leakage induction in liposomes, Figs. 8 and 9 show that the adsorption of HKH20 is significantly higher at the anionic than

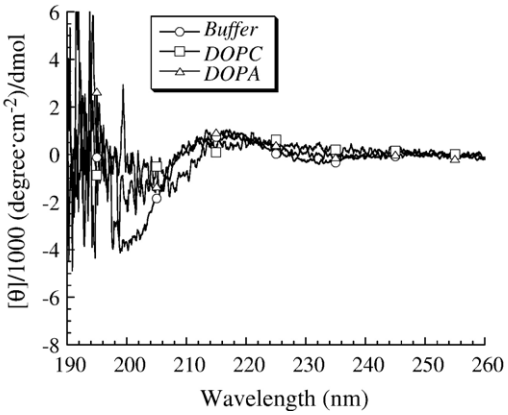

Fig. 6. Representative CD spectra for HKH20 for DOPC/cholesterol (60/40) ("DOPC") and DOPC/DOPA/cholesterol (30/30/40) ("DOPA") in 10 mM Tris buffer, pH 7.4. Similar results were obtained also for the other peptides. The helix content of the peptides investigated both in solution and when bound to the anionic and zwitterionic liposomes was in the range 2±1 to 6±2%.

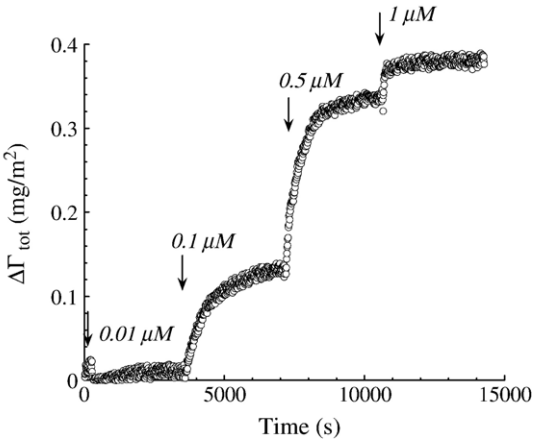

Fig. 7. Typical time-resolved adsorption of HKH20 to supported anionic bilayers consisting of DOPC/DOPA/cholesterol (30/30/40). Peptide addition and final concentration in the cuvette after addition are indicated. Background adsorption for the lipid layer (Γ=4.48±0.003 mg/m^2) is subtracted for clarity. t=0 s corresponds to the time of the first peptide addition.

at the zwitterionic supported bilayers. Furthermore, HKH20 adsorption is very low at high excess salt concentration, again in agreement with the liposome leakage experiments. Both these observations clearly indicate that electrostatics dominates the interaction between HKH20 and the lipid bilayers. Again, there is good correlation between adsorption, liposome leakage induction, and bacterial killing.

The correlation between peptide adsorption density and liposome leakage induction is somewhat less clear at first sight regarding the peptide length dependence. Thus, while liposome leakage was dramatically reduced for the three 10-amino acid truncation peptides, the adsorption of HKH10 is significantly reduced in molar terms only for the anionic lipid bilayers, and only marginally for the zwitterionic one (Figs. 8 and 9). However, since the net charge of HKH10 is only half of that of HKH20, the amount of peptide charges pinned to the membrane interface is much larger for HKH20 than for HKH10 for both the anionic and the zwitterionic membrane. Since packing defect formation and liposome leakage is expected to be critically related to the pinning of charges at the membrane surface (see below, as well as refs. [30,38]), the adsorption and the liposome leakage results are therefore consistent.

A second, at first counterintuitive, result concerns the pH dependence of HKH20 adsorption, liposome leakage induction and bacterial killing. Since HKH20 contains none less than 6 histidine residues, which as single amino acids have a pKa of 6.5, the net charge of HKH20 is essentially doubled on going from pH 7.4 (+6) to pH 5.5 (+12), not accounting counterion binding effects. In line with the reasoning above on the role of electrostatics in the action of HKH20, one might at first expect HKH20 to be more potent in liposome leakage induction and bacteria killing at the lower pH. In fact, the opposite is found for bacteria (Figs. 3 and 4) and no significant pH dependence is found regarding liposome leakage induction (Fig. 5c). Of course, changing pH is a fairly drastic measure regarding bacteria. However, both RDA (Fig. 4) and viable count analysis (Fig. 3) show that HKH20 is more efficient in killing bacteria at pH 7.4 than at pH 5.5, despite the overall bacteria viability being lower at the lower pH.

While the pH dependence observed regarding bacterial killing is of multifactorial origin and therefore not easy to interpret mechanistically, the interpretation of the lack of any significant pH dependence in liposome leakage is more straightforward. Although it could in principle be related to the higher HKH20 net charge at pH 5.5 further preventing calcein leakage as discussed above in relation to the comparison of calcein and CF leakage (CF cannot be used at pH 5.5 due to bleaching at this pH), the similarity in pH dependence for the anionic and the zwitterionic liposomes argues against such an interpretation. Instead, the (lack of) pH dependence in liposome

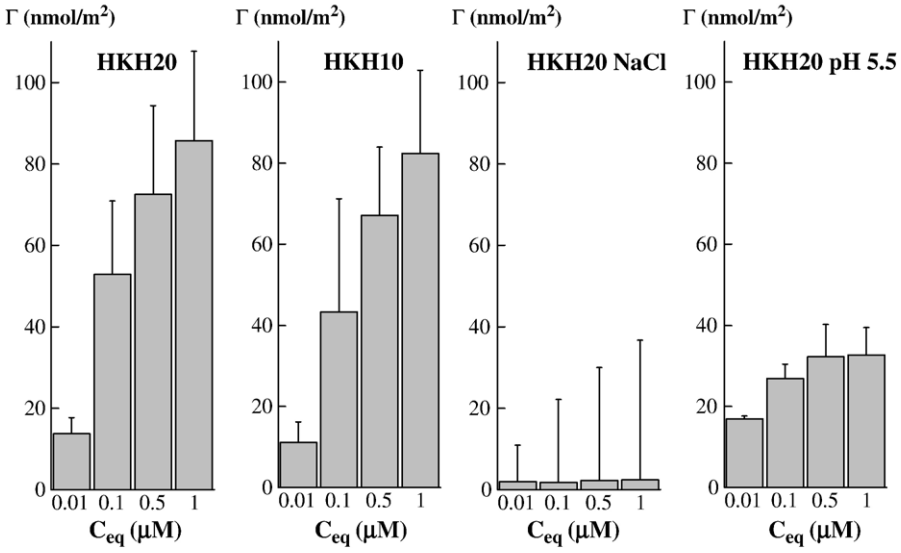

Fig. 8. Adsorption of HKH20 and HKH10 at supported DOPC/cholesterol (60/40) bilayers. The adsorption was performed from either 10 mM Tris buffer, pH 7.4, 10 mM Tris buffer plus 150 mM NaCl, pH 7.4, or 10 mM sodium acetate buffer, pH 5.5.

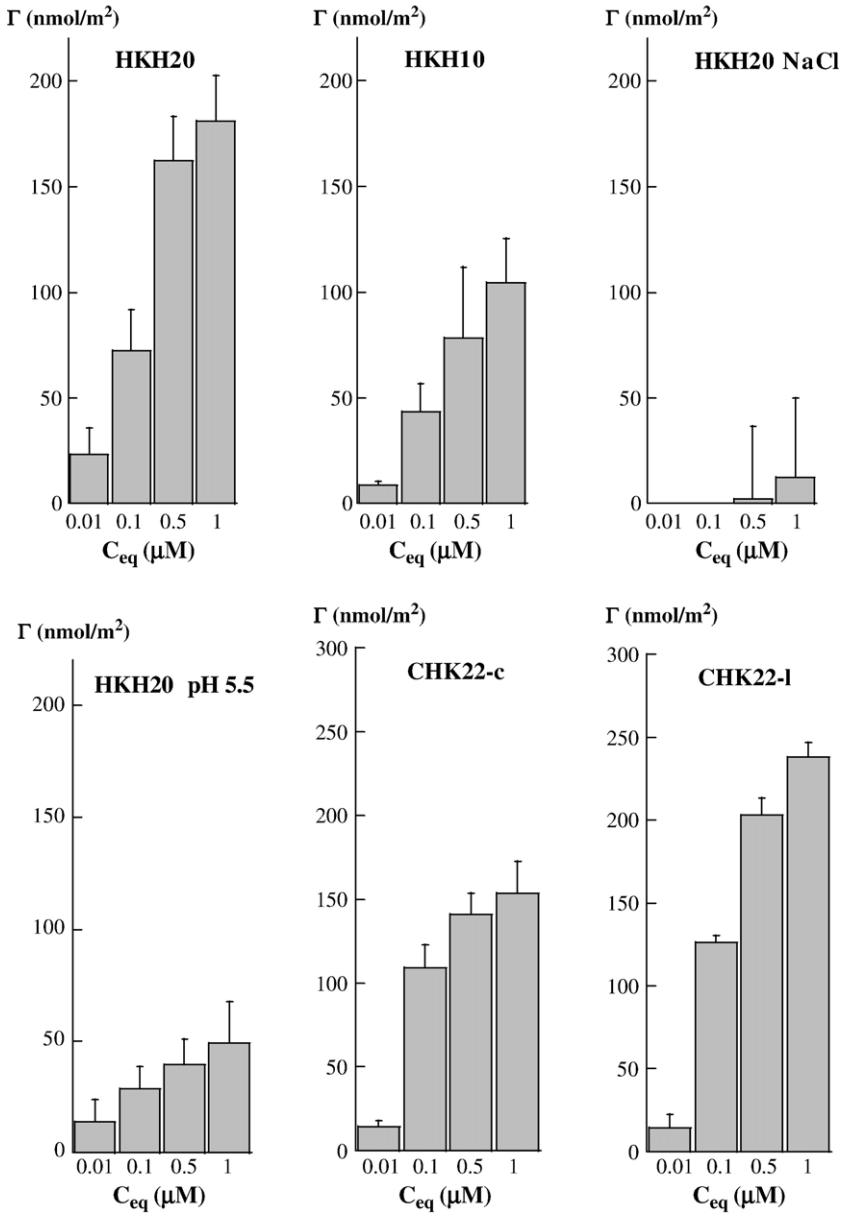

Fig. 9. Adsorption of HKH20 and HKH10 at supported DOPC/DOPA/cholesterol (30/30/40) bilayers. The adsorption was performed from either 10 mM Tris buffer, pH 7.4, 10 mM Tris buffer plus 150 mM NaCl, pH 7.4, or 10 mM sodium acetate buffer, pH 5.5. Shown also is the adsorption of CHK22 l and CHK22 c at supported DOPC/DOPA/cholesterol (30/30/40) bilayers. from 10 mM Tris buffer, pH 7.4.

leakage is most likely due to pH-dependent adsorption effects. As can be seen in Figs. 8 and 9, the adsorption of HKH20 at both anionic and zwitterionic membranes is significantly lower at pH 5.5 than at pH 7.4, in line with previous findings on reduced adsorption of polyelectrolytes and polypeptides at sufficiently high macromolecule charge densities [31–36]. In this context, it should be noted that the adsorbed peptide molecules are quite crowded, where the highest adsorbed amounts shown in Figs. 8 and 9 correspond to one peptide molecule per 18 and 37 lipid molecules for the anionic and the zwitterionic membrane, respectively. Possibly, the lack of the polarizable uncharged histidine residues in the peptide also diminishes the non-electrostatic anchoring of the peptide to the lipid membrane, contributing to the lower adsorption at pH 5.5. Counteracting this lower adsorption at low pH, however, each adsorbed HKH20 molecule carry twice the charge at pH 5.5 (Z_{net}=+12) compared to pH 7.4 (Z_{net}=+6), which renders each adsorbed peptide more efficient in membrane defect formation at the lower pH. Thus, the lower adsorption at pH 5.5 is counteracted by a more efficient membrane defect formation per adsorbed peptide molecule. Although the agreement between net number of charges adsorbed and liposome leakage induction is quantitative only in the case of the zwitterionic system, and qualitative for the anionic system, the weak pH dependence in liposome leakage is not unexpected given these two opposite pH-dependent effects.

Analogous to the lower bacterial killing displayed for the cyclic than for the linear peptide variant (Fig. 4a–b), the

liposome leakage induced by the cyclic peptide analouge is significantly lower than that of the linear variant (Fig. 4c). A similar effect was found for the zwitterionic liposome (not shown). As with the effects observed regarding peptide length and charge, this lower membrane-disruptive effect of the cyclic peptide variant is partly related to a lower adsorption, at least for the anionic bilayer (Fig. 9). (For the zwitterionic membrane, however, the saturation adsorption for the linear peptide was only ≈5% larger than that for the cyclic analogue (not shown).) Due to the connectivity of the peptide ends for the cyclic peptide, its conformational freedom is smaller than that of the linear variant. Consequently, the conformational entropy loss on adsorption is smaller for the cyclic peptide than for the linear one, which should contribute to a higher adsorption density for the cyclic peptide as compared to the linear analogue, as is the case for polymers [32,37]. The observation of the reverse behaviour shows that other factors are important in determining the peptide adsorption as well. Although not conclusively shown at this point, a reasonable interpretation of the adsorption results is that the bulky nature of the cyclic peptide prevents the peptide from penetrating into the lipid headgroup region, and hence looses some of the hydrophobic driving force for adsorption and membrane defect formation [30,38].

Although relatively scarce, there are some studies reported in literature of the effect of topology on the interaction between peptides and lipid membranes and bacteria. For example, Rosengren et al. investigated the effects of cyclization of pyrrhocoricin, and found that when using a 9 amino acid linker for cyclization of the 21 amino acid pyrrhocoicin, cyclization did not have any detrimental effect on antimicrobial potency and spectrum [39]. However, using linkers for cyclization affects not only topology but also peptide length, a crucial factor in itself for the function of antimicrobial peptides [30]. When using linker-free cyclization, a detrimental effect on peptide antimicrobial effect is generally observed. Thus, Krishnakumari et al. [40], Unger et al. [41], Rozek et al. [42], Gobbo et al. [43], and Leslie et al. [44] all found the cyclic peptide variant to be less potent in antimicrobial or liposome leakage assays than the corresponding linear peptide variant. However, the effect of peptide cyclization seems to be somewhat peptide specific regarding the bactericidal effects, as also lack of effect of cyclization was found for bovine β-defensin-2 by Krishnakumari et al. [45], as was a decreased hemolysis but retained antimicrobial activity for an analogue of tachyplesin I (forming a β-hairpin in its native form) in which all stabilising cysteines were deleted, thus rendering a linear peptide [46]. Furthermore, Unger et al. noted a decrease in antimicrobial potency of a magainin 2 analogue on cyclization, but an increased potency of a melittin analogue [41]. However, in terms of liposome leakage induction, also the latter investigation showed the cyclic variant to be less effective than the corresponding linear peptide variant for both the magainin 2 analogue and the melittin analogue. Furthermore, it was found that the main effect of cyclization in liposome systems was a decreased peptide binding to the phospholipid membrane [40]. Overall, therefore, these previous findings on the effects of peptide cyclization are in line with those found in the present investigation.

As for the peptide length dependence of bacterial killing, liposome leakage induction, and adsorption, results overall analogous to those of the present finding have been reported before [30,47]. Hence, we previously investigated consensus peptides of the type $(AKKARA)_n$ ($n=1$–4) and $(ARKAAKKA)_n$ ($n=1$–3), and found that leakage induction of both zwitterionic and anionic liposomes increased with increasing peptide length, as did peptide adsorption at supported lipid bilayers, as well as peptide-induced killing of *Enterococcus faecalis* and *Bacillus subtilis* bacteria [30]. Although the adsorption of HKH10 is significant even at conditions where liposome leakage is very marginal and hence the situation in the present peptide system is not identical to that for the consensus peptides previously investigated, the peptide length dependence effects are in overall agreement in so far that shorter peptides result in a lower number of charges localized at the lipid membrane surface, hence resulting in a lower electrostatically driven membrane defect formation. Also regarding the length dependence of the antimicrobial effects the presently reported findings are in agreement with those previously reported for consensus peptides [30], as well as with finding reported by Deslouches et al. regarding the length dependence of the antibacterial effect of a 12-residue lytic base motif peptide [47].

Regarding the effect of the peptide net charge on its bactericidal effect, liposome-disruptive capacity, and adsorption at phospholipid membranes, there are numerous studies showing that electrostatic interactions play a key role in the action of cationic AMP systems, and that decreasing the charge density of the peptide results in decreased adsorption, liposome-disruptive capacity, and bactericidal effects [30,38,48]. Also for H-containing peptides such a dependence on the peptide charge density has been observed. Thus, Makovitzki and Shai investigated the pH dependence of lipopeptides with dodecanoic acid-modified 12-mer peptides of the type LXXLLXXLLXXL, where X is H, K or R [49]. While the K- and R-containing peptides displayed little pH dependence, an H-containing one showed a pronounced pH dependence. This H-containing peptide did not display any antifungal properties at pH 7.4 (contrary to the K- and R-containing peptides), but was active at pH 5.5. Analogously, this H-containing peptide induced liposome leakage at the lower pH but not at the higher, an effect related to a higher peptide adsorption at lipid membranes at the lower pH. These results clearly demonstrate the importance of electrostatic interactions both for peptide adsorption and resulting lipid membrane rupture, and are in agreement with the reports mentioned above in which the peptide charge density was varied by composition changes rather than by pH. In fact, we have observed similar results as those reported by Makovitzki and Shai for peptides of the type $(AHHAHA)_4$ and $(AHHAAHHA)_3$, and are currently writing up a report on these findings. It should be noted, however, that these findings are not in contradiction with the pH results presently reported. Thus, there is little doubt that when increasing the net positive peptide charge from close to zero to a high value, peptide adsorption to

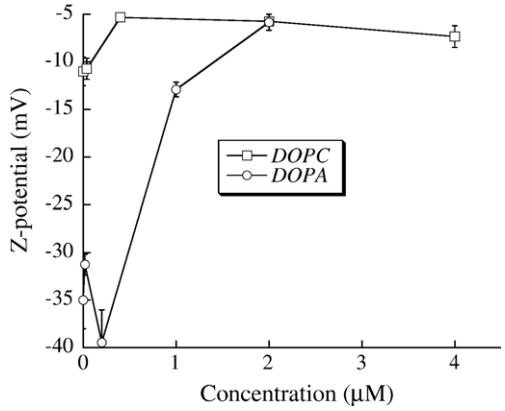

Fig. 10. z-potential for zwitterionic DOPC/cholesterol (60/40) ("DOPC") and anionic DOPA/DOPC/cholesterol (30/30/40) ("DOPA") liposomes in the presence of HKH20.

negatively charged lipid surfaces increases, as does membrane lytic effects in both liposomes and bacteria. What the presently reported data show, however, is that there is a limit to these charge-induced effects at sufficiently high peptide charge density due to a decreased peptide adsorption. Both peptide adsorption and the membrane disruptive capacity at these high charge densities are lower than those at intermediate peptide charge density, but nevertheless significantly higher than for the corresponding uncharged peptide variants.

To the best of our knowledge, there has been no report in literature showing that when the peptide charge density is sufficiently high, a decreased peptide adsorption results in a decreased liposome-disruptive capacity of the peptide. A decreased activity towards some bacteria was indeed found at very high peptide charge by Giangaspero et al., but in that case, the decreased activity was probably due to a decreased helix formation tendency of the peptide at high peptide charge, rather than the charge directly [50]. However, for both polyelectrolytes and polyampholytes, a decreased adsorption has been found at high macromolecule charge densities, primarily due to the electrostatic penalty from effectively reducing the mean distance between macromolecule charges on adsorption [31–36]. Additionally, the adsorption of both block copolymers and hydrophobe-modified proteins has been found to decrease with decreasing hydrophobic content [51,52]. Although histidin is not hydrophobic on the Eisenberg scale (−0.4), the bulky and polarizable nature of this residue renders it susceptible to incorporation into lipid bilayers, as evidenced, e.g., by the free energy of transfer from the vapor phase to an organic solvent [53]. It is therefore quite likely that the histidin residues contribute to the adsorption driving force for HKH20 at pH 7.4. Given the above, the present finding of a decreased HKH20 adsorption at pH 5.5 is not unexpected.

Since the peptides investigated are net positively charged, their adsorption reduces the net negatively electrostatic potential of the liposomes, seen e.g., in the z-potential measurements (Fig. 10). It should be noted in particular in this context that the magnitude of the z-potential at maximum leakage induction (≈5 mV) is smaller than that in the absence of peptide (≈35 mV and 10 mV for the anionic and the zwitterionic system, respectively). Thus, peptide addition results essentially in an elimination of the effective surface potential of the peptide-covered liposomes. Hence, liposome leakage is clearly *not* related to an adsorption-dependent build-up of a global electrostatic potential and resulting osmotic stress, as is the case, e.g., for some cationic surfactants [54]. Similar findings were obtained also at pH 5.5 (not shown). Furthermore, the peptide variants investigated display essentially a random coil conformation both in aqueous solution and when bound to the liposomes, hence mechanisms based on membrane-bound peptide helices observed for some AMPs [3–10,23,55] are unlikely. Moreover, since we observe no membrane thinning effects [23,56] due to peptide binding in the ellipsometry results (not shown), the most likely mechanism seems to be electrostatically driven packing defects around each adsorbed peptide molecule, or related phenomena previously discussed [23,57–59]. Further work to elucidate these mechanisms is currently underway.

4. Conclusion

Electrostatic interactions, peptide length and topology are all important for the interaction between HKH20 peptide variants and lipid membranes. In particular, shortening the peptide, making it cyclic, or reducing the electrostatic interactions reduces the membrane-disruptive capacity of the peptides. These effects are related to the adsorption of the peptide (charges) at the lipid bilayers, whereas the peptide secondary structure seems not to play an important role in the membrane defect formation. The adsorption, in turn, is dominated to electrostatic peptide–lipid interactions. Although the detailed membrane rupture mechanism is unknown at present, the results point towards the formation of local packing defects around the peptide molecules caused by the charges these carry. Good correlation is observed between peptide-induced liposome disruption and bacterial killing, indicating that lipid bilayer rupture is a key mechanism in the antibacterial action of these peptides.

Acknowledgements

Lise-Britt Wahlberg and Mina Davoudi are gratefully acknowledged for skillful experimental support. This work was supported by grants from the Swedish Research Council (projects 13471 and 621-2003-4022), the Swedish Foundation for Strategic Research, The Swedish Government Funds for Clinical Research and DermaGen AB.

References

[1] G.L. French, Clinical impact and relevance of antibiotic resistance, Adv. Drug Delivery Rev. 57 (2005) 1514–1527.
[2] P.A. Lambert, Bacterial resistance to antibiotics: modified target sites, Adv. Drug Delivery Rev. 57 (2005) 1471–1485.
[3] M. Zasloff, Antimicrobial peptides of multicellular organisms, Nature 415 (2002) 389–395.
[4] A.K. Marr, W.J. Gooderham, R.E.W. Hancock, Antibacterial peptides for

therapeutic use: obstacles and realistic outlook, Curr. Opin. Pharmacol. 6 (2006) 1–5.
[5] L. Zhang, T.J. Falla, Cationic antimicrobial peptides—an update, Expert Opin. Investig. Drugs 13 (2004) 97–106.
[6] O. Toke, Antimicrobial peptides: new candidates in the fight against bacterial infections, Biopolymers 80 (2005) 717–735.
[7] K. Lohner, S.E. Blondelle, Molecular mechanisms of membrane pertubation by antimicrobial peptides and the use of biophysical studies in the design of novel peptide antibiotics, Comb. Chem. High Throughput Screen. 8 (2005) 214–256.
[8] Y. Shai, Mode of action of membrane active antimicrobial peptides, Biopolymers 66 (2002) 236–248.
[9] N. Papo, Y. Shai, Can we predict biological activity of antimicrobial peptides from their interactions with model lipid membranes? Peptides 24 (2003) 1693–1703.
[10] B. Bechinger, K. Lohner, Detergent-like actions of linear amphipathic cationic antimicrobial peptides, Biochim. Biophys. Acta 9 (2006) 1529–1539.
[11] A. Tossi, L. Sandri, A. Giangaspero, Amphipathic, α-helical antimicrobial peptides, Biopolymers 55 (2000) 4–30.
[12] F.J. Colilla, A. Rocher, E. Mendez, γ-Purothionins: amino acid sequence of two polypeptides of a new family of thionins from wheat endosperm, FEBS Lett. 270 (1990) 191–194.
[13] E. Mendez, A. Moreno, F. Colilla, F. Pelaez, G.G. Limas, R. Mendez, F. Soriano, M. Salinas, C. de Haro, Primary structure and inhibition of protein synthesis in eukaryotic cell-free system of a novel thionin, gamma-hordothionin, from barley endosprem, Eur. J. Biochem. 194 (1990) 533–539.
[14] P. Bulet, C. Hetru, J.-L. Dimarcq, D. Hoffmann, Antimicrobial peptides in insects: structure and function, Dev. Comp. Immunol. 23 (1999) 329–344.
[15] K. De Smet, R. Contreras, Human antimicrobial peptides: defensins, cathelicidins and histatins, Biotechnol. Lett. 27 (2005) 1337–1347.
[16] T. Ganz, Defensins and other antimicrobial peptides: a historical perspective and an update, Comb. Chem. High Throughput Screen. 8 (2005) 209–217.
[17] E. Andersson Nordahl, V. Rydengård, P. Nyberg, D.P. Nitsche, M. Mörgelin, M. Malmsten, L. Björck, A. Schmidtchen, Activation of the complement system generates antibacterial peptides, Proc. Natl. Acad. Sci. U. S. A. 101 (2004) 16884–16897.
[18] E. Andersson Nordahl, V. Rydengård, M. Mörgelin, A. Schmidtchen, Domain 5 of high molecular weight kininogen is antibacterial, J. Biol. Chem. 41 (2005) 34832–34839.
[19] M. Malmsten, M. Davoudi, A. Schmidtchen, Bacterial killing by heparin-binding peptides from PRELP and thrombospondin, Matrix Biol. 25 (2006) 294–300.
[20] K.A. Brogden, Antimicrobial peptides: pore formers or metabolic inhibitors in bacteria? Nat. Microbiol. 3 (2005) 238–250.
[21] L. Zhang, J. Parente, S.M. Harris, D.E. Woods, R.E.W. Hancock, T.J. Falla, Antimicrobial peptide therapeutics for cystic fibrosis, Antimicrob. Agents Chemother. 49 (2005) 2921–2927.
[22] V. Nizet, Antimicrobial peptide resistance mechanisms of human bacterial pathogens, Curr. Issues Mol. Biol. 8 (2006) 11–26.
[23] D.A. Steinberg, M.A. Hurst, C.A. Fujii, A.H. Kung, J.F. Ho, F.C. Cheng, D.J. Loury, J.C. Fiddes, Protegin-1: a broad-spectrum, rapidly microbicidal peptide with in vivo activity, Antimicrob. Agents Chemother. 41 (1997) 1738–1742;
U.H.N. Dürr, U.S. Sudheendra, A. Ramamoorthy, LL-37, the only human member of the cathelicidin family of antimicrobial peptides, Biochim. Biophys. Acta 1758 (2006) 1408–1425;
H.W. Huang, Molecular mechanism of antimicrobial peptides: the origin of cooperativity, Biochim. Biophys. Acta 1758 (2006) 1292–1302;
D.I. Chan, E.J. Prenner, H.J. Vogel, Tryptophan- and arginine-rich antimicrobial peptides: structures and mechanisms of action, Biochim. Biophys. Acta 1758 (2006) 1184–1202;
X. Chen, Z. Chen, SFG studies on interactions between antimicrobial peptides and supported lipid bilayers, Biochim. Biophys. Acta 1758 (2006) 1257–1273;
R. Volinsky, S. Kolusheva, A. Berman, R. Jelinek, Investigation of antimicrobial peptides in planar film systems, Biochim. Biophys. Acta 1758 (2006) 1393–1407;
T. Sigurdadottir, P. Andersson, M. Davoudi, M. Malmsten, A. Schmidtchen, M. Bodelsson, In silico identification and biological evaluation of antimicrobial peptides based on human cathelicidin LL-37, Antimicrob. Agents Chemother. 50 (2006) 2983–2989;
M.J. Nell, G.A. Tjabringa, A.R. Wafelman, R. Verrijk, P.S. Hiemstra, J.W. Drijfhout, J.J. Grote, Development of novel LL-37 derived antimicrobial peptides with LPS and LTA neutralizing and antimicrobial activities for therapeutic application, Peptides 27 (2006) 649–660.
[24] R.I. Lehrer, M. Rosenman, S.S. Harwig, R. Jackson, P. Eisenhauer, Ultrasensitive assays for endogenous antimicrobial polypeptides, J. Immunol. Methods 137 (1991) 167–173.
[25] N. Greenfield, Computed circular dichroism spectra for the evaluation of protein conformation, Biochemistry 8 (1969) 4108–4116.
[26] H. Sjögren, S. Ulvenlund, Comparison of the helix-coil transition of a titrating polypeptide in aqueous solution and at the air–water interface, Biophys. Chem. 116 (2005) 11–21.
[27] R.M.A. Azzam, N.M. Bashara, Ellipsometry and Polarized Light, North Holland Publishing Company, Amsterdam, 1989.
[28] J.A. de Feijter, J. Benjamins, F.A. Veer, Ellipsometry as a tool to study the adsorption of synthetic and biopolymers at the air–water interface, Biopolymers 17 (1978) 1759–1772.
[29] F. Tiberg, I. Harwigsson, M. Malmsten, Formation of model lipid bilayers at the silica–water interface by co-adsorption with non-ionic dodecyl maltoside surfactant, Eur. Biophys. J. 29 (2000) 196–203.
[30] L. Ringstad, A. Schmidtchen, M. Malmsten, Effect of peptide length on the interaction between consensus peptides and DOPC/DOPA bilayers, Langmuir 22 (2006) 5042–5050.
[31] M. Malmsten, Biopolymer at Interfaces, Marcel Dekker, New York, 2003.
[32] G.J. Fleer, M.A. Cohen Stuart, J.M.H.M. Scheutjens, T. Cosgrove, B. Vincent, Polymers at Interfaces, Chapman & Hall, London, 1993.
[33] N.G. Hoogeveen, M.A. Cohen Stuart, G.J. Fleer, Polyectrolyte adsorption on oxides, J. Colloid Interface Sci. 182 (1996) 133–145.
[34] M.A. Cohen Stuart, C.W. Hoogendam, A. de Keizer, Kinetics of poly-electrolyte adsorption, J. Phys.: Condens. Matter 9 (1997) 7767–7783.
[35] J. Blaakmeer, M.A. Cohen Stuart, G.J. Fleer, The adsorption of polyampholytes on negatively and positively charged polystyrene latex, J. Colloid Interface Sci. 140 (1990) 314–325.
[36] B. Mahltig, R. Jerome, M. Stamm, Diblock polyampholytes at the silicon/water interface: adsorption at various modified silicon substrates, Phys. Chem. Chem. Phys. 3 (2001) 4371–4375.
[37] A. Patel, T. Cosgrove, J.A. Semlyen, Studies of cyclic and linear poly (dimethylsiloxanes):30. Adsorption studies on silica in solution, Polymer 32 (1991) 1313–1317.
[38] L. Ringstad, E. Andersson Nordahl, A. Schmidtchen, M. Malmsten, Composition effect on peptide interaction with lipids and bacteria: variants of C3a peptide CNY21, Biophys. J. 92 (2007) 87–98.
[39] K.J. Rosengren, U. Göransson, L. Otvos, D.J. Craik, Cyclization of pyrrhocoricin retains structural elements crucial for the antimicrobial activity of the native peptide, Biopolymers 76 (2004) 446–458.
[40] V. Krishnakumari, A. Sharadadevi, N. Sitaram, R. Nagaraj, Consequences of introducing a disulfide bond into an antibacterial and hemolytic peptide, J. Peptide Res. 54 (1999) 528–535.
[41] T. Unger, Z. Oren, Y. Shai, The effect of cyclization of magainin 2 and melittin analogues on structure, function, and model membrane interactions: implications to their mode of action, Biochemistry 40 (2001) 6388–6397.
[42] A. Rozek, J.-P.S. Powers, C.L. Friedrich, R.E.W. Hancock, Structure-based design of an indolicidin peptide analogue with increased protease stability, Biochemistry 42 (2003) 14130–14138.
[43] M. Gobbo, L. Biondi, F. Filira, R. Gennaro, M. Benincasa, B. Scolaro, R. Rocchi, Antimicrobial peptides: synthesis and antibacterial activity of linear and cyclic drosocin and apidaecin 1b analogues, J. Med. Chem 45 (2002) 4494–4504.
[44] D.B. Leslie, P.S. Viezen, V. Lazaron, K.R. Wasiluk, D.L. Dunn, Comparison of endotoxin antagonism of linear and cyclic peptides derived

from Limulus and anti-lipopolysaccharide factor, Surg. Inf. 7 (2006) 45–52.
[45] V. Krishnakumari, A. Sharadadevi, S. Singh, R. Nagaraj, Single disulfide and linear analogues corresponding to the carboxy-terminal segment of bovine β-defensin-2: effects of introducing the β-hairpin nucleating sequence D-Pro-Gly on antibacterial activity and biophysical properties, Biochemistry 42 (2003) 9307–9315.
[46] A. Ramamoorthy, S. Thennarasu, A. Tan, K. Gottipati, S. Sreekumar, D.L. Heyl, F.Y.P. An, C.E. Shelburne, Deletion of all cysteines in Tachyplesin I abolishes hemolytic activity and retains antimicrobial activity and lipopolysaccharide selective binding, Biochemistry 45 (2006) 6529–6540.
[47] B. Deslouches, S.M. Phadke, V. Lazarevic, M. Cascio, K. Islam, R.C. Montelaro, T.A. Mietzner, De novo generation of cationic antimicrobial peptides: influence of length and tryptophan substitution on antimicrobial activity, Antimicrob. Agents Chemother. 49 (2005) 316–322.
[48] I.H. Lee, Y. Cho, R.I. Lehrer, Effects of pH and salinity on the antimicrobial properties of clavanins, Infect. Immun. 65 (1997) 2898–2903.
[49] A. Makovitzki, Y. Shai, pH-Dependent antifungal lipopeptides and their plausible mode of action, Biochemistry 44 (2005) 9775–9784.
[50] A. Giangaspero, L. Sandri, A. Tossi, Amphipathic α helical antimicrobial peptides: a systematic study of the effects of structural and physical properties on biological activity, Eur. J. Biochem. 268 (2001) 5589–5600.
[51] M. Malmsten, A. Veide, Effects of amino acid composition on protein adsorption, J. Colloid Interface Sci. 178 (1996) 160–167.
[52] M. Malmsten, N. Burns, A. Veide, Electrostatic and hydrophobic effects of oligopeptide insertions on protein adsorption, J. Colloid Interface Sci. 204 (1998) 104–111.
[53] A. Radzicka, R. Wolfenden, Comparing the polarities of amino acids: side-chain distribution coefficients between vapor phase, cyclohexane, 1-octanol, and neutral aqueous solution, Biochemistry 27 (1988) 1664–1670.
[54] J. Gustafsson, G. Orädd, M. Almgren, Disintegration of the lecithin lamellar phase by cationic surfactants, Langmuir 13 (1997) 6956–6963.
[55] F. Porcelli, B. Buck, D.-K. Lee, K.J. Hallock, A. Ramamoorthy, G. Veglia, Structure and orientation of paradaxin determined by NMR experiments in model membranes, J. Biol. Chem. 279 (2004) 45815–45823.
[56] A. Mecke, D.-K. Lee, A. Ramamoorthy, B.G. Orr, M.M.B. Holl, Membrane thinning due to antimicrobial peptide binding: an atomic force microscopy study of MSI-78 in lipid bilayers, Biophys. J. 89 (2005) 4043–4050.
[57] A. Tennarasu, D.-K. Lee, A. Poon, K.E. Kawulka, J.C. Vederas, A. Ramamoorthy, Membrane permeabilization, orientation, and antimicrobial mechanism of subtilosin A, Chem. Phys. Lipids 137 (2005) 38–51.
[58] A. Ramamoorthy, S. Thennarasu, D.-K. Lee, A. Tan, L. Maloy, Solid-state NMR investigation of the membrane-disrupting mechanism of antimicrobial peptides MSI-78 and MSI-594 derived from magainin 2 and melittin, Biophys. J. 91 (2006) 206–216.
[59] S. Thennarasu, D.-K. Lee, A. Tan, U.P. Kari, A. Ramamoorthy, Antimicrobial activity and membrane selective interactions of a synthetic lipopeptide MSI-843, Biochim. Biophys. Acta 1711 (2005) 49–58.